Nonequilibrium α emission in deeply inelastic $^{16}O + {}^{58}Ni$ collisions at 6 and 9 MeV/nucleon

H. Ho, P. L. Gonthier,* G.-Y. Fan,† W. Kühn,‡ A. Pfoh, L. Schad, R. Wolski,§ and J. P. Wurm
Max-Planck-Institut für Kernphysik, D-6900 Heidelberg, Federal Republic of Germany

J. C. Adloff, D. Disdier, A. Kamili, V. Rauch, G. Rudolf, F. Scheibling, and A. Strazzeri
Centre de Recherches Nucleaires, Strasbourg, France
(Received 30 March 1982)

Energy and angular correlations of α particles in coincidence with deeply inelastic ejectiles from $^{16}O + {}^{58}Ni$ collisions at 6 and 9 MeV/nucleon reveal α emission processes which cannot be explained by sequential emission from the fragments.

[NUCLEAR REACTIONS $^{58}Ni(^{16}O,HI\alpha)$, $E = 6,9$ MeV/nucleon; energy and angular correlation for HI α coincidences measured; deduced reaction mechanism.]

Recently, a study on heavy-ion-α-particle correlation[1] cast doubt on the existence of nonequilibrium α emission in deeply inelastic $^{16}O + {}^{58}Ni$ collisions at 6 MeV/nucleon.[2] Assuming sequential α emission from the primary projectilelike and targetlike fragments, a model calculation was applied in Ref. 1 to earlier correlation data on $^{16}O + {}^{58}Ni$ at 6 MeV/nucleon (Ref. 2), and it was found that the model calculation completely exhausts the observed yields. It was claimed that the strongly forward peaked angular correlation observed in Ref. 2 can be entirely explained by sequential α emission from the projectilelike fragment. However, the calculations in which the collision of the primary fragments and the subsequent decay by light particle emission were simulated[1] were based on imprecise information about the energy and angular distribution of the primary fragments, as well as the decay energy distribution of emitted light particles. In this paper we report on the measurement of the primary fragment distribution, directly giving reliable parameters for such calculations. A further improvement was achieved by angular correlations measured with narrow steps between neighboring α detection angles and extended to much more forward angles than in a previous study.[2] Owing to that, structures in the angular correlations are visible that are not observed in most other studies. The two steps enabled us to fractionate α emission into sequential emission from the fragments and nonequilibrium emission. In an additional experiment at a higher bombarding energy, the heavy ion was detected at a large backward angle, and the same nonequilibrium component was observed. The current study confirms the observation of nonequilibrium α emission in an earlier study,[2] but shows that owing to the lack of forward angle data, the contribution of nonequilibrium α emission was overestimated. On the other hand, the two measurements at 6 and 9 MeV/nucleon show that the multiplicity for the nonequilibrium component increases strongly with bombarding energy, in agreement with the high multiplicity values measured for the $^{16}O + Ti$ system at 20 MeV/nucleon.[5,11]

The experiments had been performed with a 96 MeV ^{16}O beam supplied by the MP tandem Van de Graaff accelerators in Heidelberg and Strasbourg, and with a 147 MeV postaccelerated ^{16}O beam in Heidelberg. ΔE-E telescopes were used to measure charge and energy of heavy ions and light particles. To lower the detection threshold for light particles, in addition, their time of flight was measured in the experiment at 147 MeV. In order to study α emission from the projectilelike fragments, a special detector setup was used: two position sensitive telescopes each consisting of a gas ionization ΔE detector and a position sensitive Si E detector of 50×8 mm^2 (100×8 in some experiments) sensitive area were mounted with their larger (position sensitive) extension paralleled. Since the telescopes' position sensitive extensions were also parallel to the horizontal plane containing the beam axis, they measured simultaneously light particles and heavy ions in the same range of scattering angles. The angular ranges

were (15°,40°), (26°,64°), and (30°,75°). The separation between the telescopes in the direction perpendicular to the horizontal plane was ~5°, allowing us to detect heavy-ion-α-particle coincidences with differences in detection angle as small as 5°. Under such conditions α emission from the projectilelike fragment has two kinematical solutions, of which the high α energy solution is as well separated from the low α energy solution as from α emission from the targetlike fragment.[2] The targets were isotopically enriched ^{58}Ni foils of 1 mg/cm^2. In order to be able to discriminate reactions with light target contaminations, carbon target measurements were performed for almost all α detection angles. From these measurements lower limits for heavy ion energies were derived which reduced possible contributions from reactions with light target contaminations to less than 10% for every α detection angle. These small contributions were not subtracted in the data. At 96 MeV an upper limit in the heavy ion energy was set in order to select the deeply inelastic component. Assuming simple two-body kinematics, these limits correspond to a range of two-body Q values of (−25,−42) MeV and (−29,−45) MeV for oxygen and carbon coincidences, respectively. At 147 MeV the lower limits correspond to −93 and −85 MeV, respectively. All energy signals and time of flight differences for heavy-ion-light-particle coincidences were digitized and recorded on line on magnetic tape event by event and analyzed off line. Random events contributed less than 15% and were subtracted in all data presented.

Figure 1 shows in-plane angular correlations for α particles in coincidence with deeply inelastic carbon (dots) and oxygen (circles) detected at $\theta_{HI}^{L} = -35°$ for the $^{16}O + ^{58}Ni$ system at 96 MeV. We have plotted the differential α multiplicity, i.e., the number of α particles per deeply inelastic scattered heavy ion and per unit solid angle, versus the α detection angle in the laboratory system θ_{α}^{L}. The angular correlations show distinct structure in the forward region and extend to much more forward angles than earlier data presented.[2] It can be clearly visualized that in the angular region of ±40° around the detected heavy ion, structures show up that could be ascribed to α emission from projectilelike fragments. Since these structures are observed in coincidence with carbon and oxygen, one has deeply inelastic collisions producing excited oxygen and neon fragments followed by sequential α decay of the fragments. This is different in studies where such structures are observed in coincidence with quasielastic fragments but not with fragments with the projectile charge.[3,4] Using the close-geometry setup, we have investigated α emission from the projectilelike fragments in more detail. Selecting the high energy solution of the α decay, the distribution of the relative energy between the α particle and the secondary fragment was constructed and studied as a function of scattering angle of the primary fragment. In the following we demonstrate the basic features of the analysis for deeply inelastic primary oxygen, i.e., for three-body Q values < -14 MeV.

Relative energy distributions were constructed from carbon-α-particle coincidences and are displayed in Fig. 2 (left side) for three primary oxygen angles 20°, 40°, and 60°. One can see that there are practically no events with relative energies larger than 8 MeV. The relative energy distributions have a most probable energy of 3.5 MeV with a width of 2.5 MeV. The pronounced peaks at 3 and 4 MeV relative energy—visible at most angles— can be

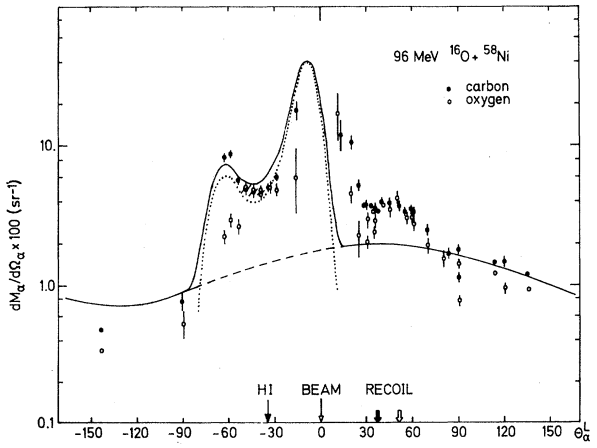

FIG. 1. In-plane angular correlation for α particles in coincidence with deeply inelastic carbon (dots) and oxygen (circles) detected at 35° for 96 MeV $^{16}O + ^{58}Ni$. Curves drawn are results of simulation calculations.

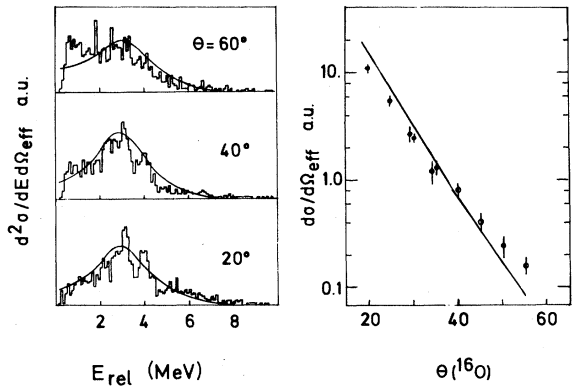

FIG. 2. Relative energy distributions (left side) and angular distributions (right side) for primary oxygen decaying by α emission. Curves drawn are results of simulation calculations.

identified with 4^+ states in ^{16}O at 10.4 and 11.1 MeV excitation energy and a 2^+ state at 11.5 MeV. Integrating over the relative energy distribution for the various primary oxygen angles, we obtain the primary oxygen angular distribution as shown in Fig. 2 (right side). It turns out that the kinetic energy and the slope of the primary oxygen decaying by α emission are close to those for deeply inelastic oxygen from singles measurements. The energy and angular distributions of the primary fragments and the relative energy between the decay products are essential ingredients in calculations where the deeply inelastic collision of the primary fragments and the subsequent deexcitation by light particle emission is simulated. The full curves in Fig. 2 show results of such calculations where the Q value distribution of deeply inelastic primary oxygen and the distribution of the relative energy were described by Gaussian distributions. For the angular distribution of deeply inelastic primary oxygen, $d\sigma/d\Omega$, an exponential function decreasing with scattering angle in the center of mass and isotropy for the α decay of oxygen were used. It was found that the parameters of the Gaussian distribution were independent of the primary oxygen angle. The non-Gaussian shape of the relative energy spectra (Fig. 2) is due to the energy dependence of the detection efficiency and is closely reproduced by the calculation. It should be stressed at this point that in the measurement of α emission from $^{16}O^*$ we cannot *a priori* discriminate $^{20}Ne^*$ decaying by two succeeding α emissions to ^{12}C. Such contributions—if any—show up as continuous background in the relative energy spectra, and it was checked that inclusion of such contributions in the simulation calculation does not change the results significantly.

The dotted curve in Fig. 1 is a calculation simulating α emission from quasielastic and deeply inelastic primary oxygen. It can explain most of the observed structure around the detected heavy ion, but, however, fails to describe the high yield observed at 7° and 15° on the opposite side of the beam. Relative energy distributions with a most probable energy of 5.5 MeV and a width of 8.3 MeV are necessary to fit the peak in beam direction. This, however, is in contradiction to the breakup data measured at 20°. The data on the opposite side fall off steeply until 25° and moderately from there on. Performing a calculation for α emission from the targetlike fragment with the parameters adjusted at the coincident α and heavy ion energy spectra measured for $\theta_\alpha^L=80°$ to 140°, we obtain the dashed curve in Fig. 1. The sum of sequential α emission from both fragments (the full curve in Fig. 1) cannot describe the data. Apart from an unexplained yield close to the beam direction, there also persists an excess yield in the direction of the recoiling targetlike fragment. The recoil direction is marked in Fig. 1 by the full and the open arrow for carbon and oxygen coincidences, respectively. Using results from out-of-plane measurements we can integrate over the sphere and obtain the following multiplicities for α particles: (i) from the projectilelike fragment, $M_\alpha=0.14\pm0.04$, (ii) from the targetlike fragment, $M_\alpha=0.10\pm0.03$, and (iii) in the excess, $M_\alpha=0.02\pm0.01$. We have to interpret the multiplicity values in the following way: Since we have tried to explain the correlation data with the maximum amount of sequential emission, a minimum amount for the excess yield results.

In order to obtain more information about the excess yield we have performed another heavy-ion-light-particle correlation experiment. The main emphasis in this latter experiment was to change the dynamics of the heavy ion collision by (i) increasing the bombarding energy and (ii) detecting the heavy ion at a large scattering angle. Figure 3 shows the angular correlation for α particles in coincidence with carbon (dots) and oxygen (circles) detected at $\theta_{HI}^L=-60°$ for the system $^{16}O+{}^{58}Ni$ at 147 MeV. Since at this bombarding energy the grazing angle is 15°, we observe only deeply inelastic scattered fragments. The α detection angles are not as closely spaced as in Fig. 1, but one can recognize the same pattern except for an overall shift of $-30°$. Again, the simulation calculation (full curve), composed of α emission from the projectilelike fragment (dotted curve) and from the targetlike fragment (dashed curve), cannot describe the angular correlation. From the α correlation angles $\theta_\alpha^L=-45°$ and $-75°$, the relative energy distribution for α emission from the projectilelike fragments was determined and a larger mean of 5.5 MeV and a larger width of 4.7

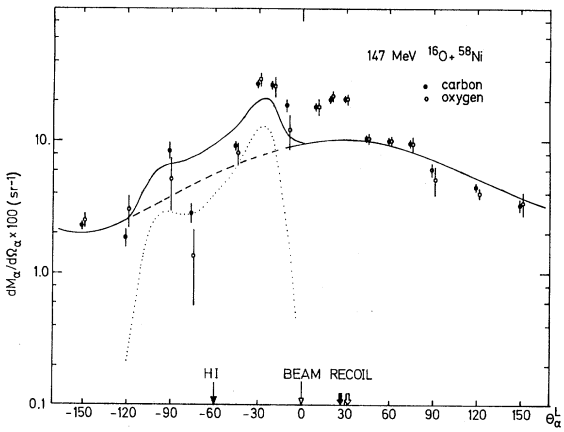

FIG. 3. Same as Fig. 1, but for heavy ions detected at 60° and 147 MeV $^{16}O+{}^{58}Ni$.

MeV were found. Similar relative energy distributions are observed in 310 MeV $^{16}O+^{197}Au$ reactions[3] and indicate that these distributions do not change significantly above 147 MeV bombarding energy. Assuming similar out-of-plane anisotropies as measured at 96 MeV, we estimate the multiplicity for α particles (i) from the projectilelike fragment to $M_\alpha = 0.04 \pm 0.01$, (ii) from the targetlike fragment to $M_\alpha = 0.53 \pm 0.16$, and (iii) in the excess to $M_\alpha = 0.09 \pm 0.05$.

Further information comes from the spectra in the direction of the recoiling targetlike fragment. Figure 4 shows α energy spectra measured at 45° (top) and 20° (bottom) for 96 and 147 MeV, respectively, in coincidence with deeply inelastic carbon. The dotted curve is the expectation for sequential emission from deeply inelastic scattered fragments. One sees that sequential emission cannot reproduce the high and low energy parts of the spectra. The excess yield at low energies is due to reactions with light target contamination, as was checked with carbon target measurements. The excess yield at higher α energies is drawn in Fig. 4 as a smooth dashed curve, whereas the full curve represents the sum of sequential emission and excess yield. At all angles where excess yield is observed, we find the same broad energy distribution for the excess yield with the most probable energy higher than the energy for sequential α particles from the targetlike fragment but lower than the energy for α particles with beam velocity (indicated by V_{BEAM}). In order to explain the highly energetic α particles by sequential emission from projectilelike fragments, we have to assume relative energies of ~ 25 and ~ 35 MeV for 6 and 9 MeV/nucleon bombarding energy, respectively, and primary fragment energies which are more than a factor of 2 lower than normal deeply inelastic fragment energies. Reviewing all the experimental facts, we are unable to explain all data by statistical emission from fully accelerated fragments.

On the other hand, the assumption of emission from fully accelerated fragments is not strictly true, and for higher excitation energies of the fragments, some fraction of the statistical α particles is emitted before the fragments are fully accelerated. To study the effect of proximate fragments we performed three-body-Coulomb-trajectory calculations with the assumption that before scission the two fragments rotate as sticking spheres with a total angular momentum of $45\hbar$ (Ref. 8) in the same direction as results from a negative deflection function.[9] After scission we assume that the fragments decay statistically, according to the exponential decay law, by α emission with the radial kinetic energy distribution governed by a temperature of 2 MeV. It turns out that even for very short lifetimes of the projectilelike fragments, α emission from these fragments cannot explain the excess yield unless we assume unrealistically high decay energies. For α emission from the targetlike fragment, calculated angular correlations are shown in Fig. 5 for various lifetimes. As can be seen, proximity effects manifest themselves by a shadow in the direction of the detected carbon and by some buildup of yield at the edges of the shadow. Indeed, we may interpret the low yield at $\theta_\alpha^L = -75°$ in Fig. 3 as an indication of shadowing,[6] but we also see that the calculated buildup of yield in the recoil direction is too small to explain the experimentally observed excess yield.

We therefore conclude that statistical emission from the fragments cannot explain the excess yield of α particles and that these α particles have to be emitted during interaction of the two fragments. From Fig. 5 we infer that α emission from the targetlike fragment could account for the excess yield if we were to ignore the concept of isotropic emission in the restframe of the targetlike fragment: A

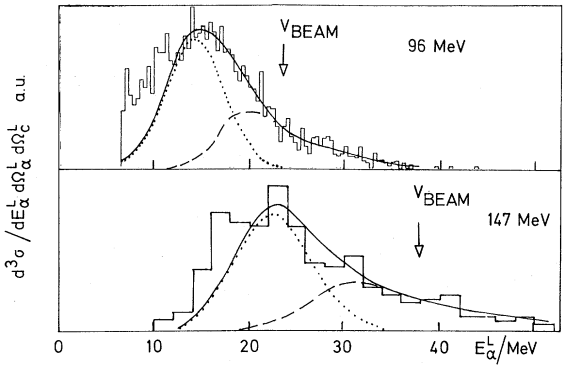

FIG. 4. Coincident α energy spectra measured at 45° (top) and 20° (bottom) for 96 and 147 MeV bombarding energy, respectively. The dotted curve is the contribution from sequential emission, the dashed curve represents the excess yield, and the full curve is the sum of both.

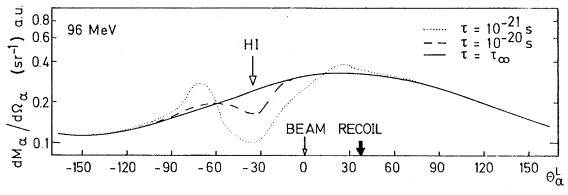

FIG. 5. Calculated in-plane angular correlation for α particles emitted from the targetlike fragment including proximity effects between α particles and the projectilelike fragment. The curves represent different lifetimes of the targetlike fragments, τ, with $\tau = \tau_\infty$ corresponding to emission from fully accelerated fragments.

localized region on the nuclear surface with higher emission probability for highly energetic α particles could account for all experimental facts, as has already been proposed in earlier studies.[2,10] On the other hand, the observation that the excess yield is focused into a small angular region and that the mean velocity is close to beam velocity supports the explanation of α emission in the first stages of heavy ion collision followed by deeply inelastic collision of the residual fragments.[5,7] To discriminate between the two processes at these low bombarding energies is not as easy as it was in the system $^{16}O + Ti$ at 310 MeV.[5] There, both processes have been observed separately since their energy distributions are sufficiently different at high bombarding energy. In order to trace the evolution of these two processes as a function of bombarding energy, it is desirable to perform similar studies in the range of 10 to 20 MeV/nucleon.

In conclusion, we have reconfirmed our earlier study[2] that nonequilibrium α emission exists in $^{16}O + ^{58}Ni$ collisions at 6 MeV/nucleon. In contrast to other studies, our simulation calculations are based on the direct measurement of the α decaying primary fragments leaving no free parameter for the calculation. The multiplicity of nonequilibrium α particles was found to increase from 0.02 ± 0.01 to 0.09 ± 0.05 for bombarding energies from 6 to 9 MeV/nucleon. This trend is confirmed by similar detailed analyses applied to heavy-ion-α-particle correlation data measured for the systems ^{32}S, $^{40}Ar + ^{93}Nb$ at 10 MeV/nucleon[6,12] and $^{16}O + Ti$ at 20 MeV/nucleon.[5,11] We have plotted in Fig. 6 the multiplicity of nonequilibrium α particles, M_α^{ne}, deduced from these various systems as a function of the relative velocity between projectile and target at the barrier B

$$[B = Z_p Z_t e^2/R,\ R = 1.22(A_p^{1/3} + A_t^{1/3}) + 2.0] .$$

The exponential increase of the multiplicity with the relative velocity clearly shows that although nonequilibrium processes contribute at the percentage level at low bombarding energy, they cannot be neglected at medium and high bombarding energies.

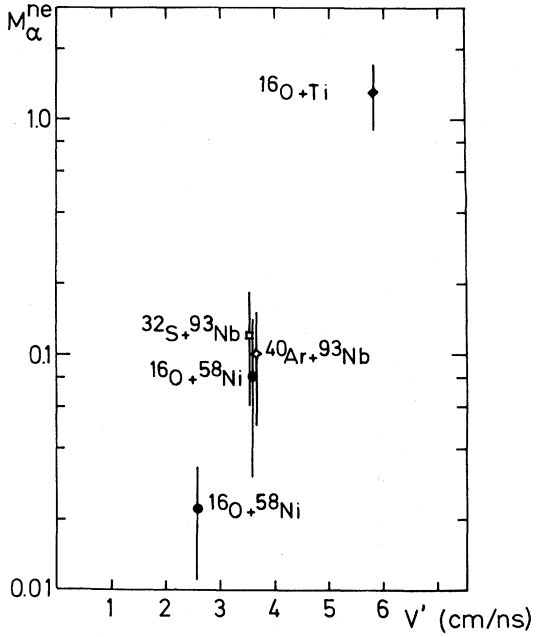

FIG. 6. Multiplicity of nonequilibrium α particles as a function of relative velocity between projectile and target at the barrier for several systems.

*Present address: Cyclotron Institute, Texas A&M University, College Station, TX 77840.

†Permanent address: Institute of Modern Physics, Academia Sinica, Lanchow, China.

‡Present address: Argonne National Laboratory, Argonne, IL 60439.

§Permanent address: Institute of Nuclear Physics, Krakow, Poland.

[1]G. R. Young, R. L. Ferguson, A. Gavron, D. C. Hensley, F. E. Obenshain, F. Plasil, A. H. Snell, M. P. Webb, C. F. Maguire, and G. A. Petitt, Phys. Rev. Lett. 45, 1389 (1980).

[2]H. Ho, R. Albrecht, W. Dünnweber, G. Graw, S. G. Steadman, J. P. Wurm, D. Disdier, V. Rauch, and F. Scheibling, Z. Phys. A 283, 235 (1977).

[3]M. Bini, C. K. Gelbke, D. K. Scott, T. J. Symons, P. Doll, D. L. Hendrie, J. L. Laville, J. Mahoney, M. C. Mermaz, C. Olmer, K. van Bibber, and H. H. Wieman, Phys. Rev. C 22, 1945 (1980).

[4]A. Gamp, M. Bürgel, M. R. Clover, C. Egelhaaf, H. Fuchs, B. Gebauer, H. Homever, and J. C. Jacmart, Z. Phys. A 300, 63 (1981).

[5]H. Ho, P. Gonthier, M. N. Namboodiri, J. B. Natowitz, L. Adler, S. Simon, K. Hagel, R. Terry, and A. Khodai, Phys. Lett. 96B, 51 (1980).

[6]H. Ho, in *Proceedings of the Symposium on Deep-Inelastic and Fusion Reactions with Heavy Ions, Berlin, 1979,* edited by W. von Oertzen (Springer, Berlin, 1980).

[7]R. K. Bhowmik, E. C. Pollaco, N. E. Sanderson, J. B. A. England, and C. C. Morrison, Phys. Rev. Lett. 43, 619 (1979).

[8]H. Ho, R. Albrecht, H. Damjantschitsch, F.-J. Demond, W. Kühn, J. Slemmer, J. P. Wurm, D. Disdier, V. Rauch, F. Scheibling, and T. Døssing, Z. Phys. A 300, 205 (1981).

[9]C. Lauterbach, W. Dünnweber, G. Graw, W. Hering, H. Puchta, and W. Trautmann, Phys. Rev. Lett. 41, 1774 (1978).

[10]R. Weiner and M. Weström, Nucl. Phys. A286, 282 (1977); P. A. Gottschalk and M. Weström, *ibid.* A314, 232 (1979).

[11]P. L. Gonthier, H. Ho, M. N. Namboodiri, J. B. Natowitz, L. Adler, S. Simon, K. Hagel, R. Terry, and A. Khodai (unpublished).

[12]G.-Y. Fan, H. Ho, P. L. Gonthier, W. Kühn, A. Pfoh, L. Schad, R. Wolski, J. P. Wurm, J. C. Adloff, D. Disdier, V. Rauch, and F. Scheibling Z. Phys. A (to be published).